Available online at www.sciencedirect.com
SCIENCE DIRECT®
Catalysis Today xxx (2005) xxx–xxx
CATALYSIS TODAY
www.elsevier.com/locate/cattod

Application of transition path sampling methods in catalysis: A new mechanism for C −C bond formation in the methanol coupling reaction in chabazite

Cynthia S. Lo [a], Ravi Radhakrishnan [b], Bernhardt L. Trout [a,*]

[a] *Department of Chemical Engineering, Massachusetts Institute of Technology, 77 Massachusetts Avenue, Room 66-458, Cambridge, MA 02139, USA*
[b] *Department of Bioengineering, University of Pennsylvania, 120 Hayden Hall, 3320 Smith Walk, Philadelphia, PA 19104, USA*

Abstract

We describe the application of transition path sampling methods to the methanol coupling reaction in the zeolite chabazite; these methods have only been recently applied to complex chemical systems. Using these methods, we have found a new mechanism for the formation of the first C −C bond. In our mechanism, the reaction, at 400 °C, proceeds via a two-step process: (1) the breaking of the C −O bond of the chemisorbed methoxonium cation, followed by the transfer of a hydride ion from the remaining methanol molecule to the methyl cation, resulting in the formation of H_2O, CH_4, and CH_2OH^+ and (2) a simultaneous proton transfer from methane to water, and direct C −C bond formation between the methyl anion and CH_2OH^+, resulting in the formation of ethanol. The C −C bond forming process has the higher barrier, with an activation energy of about 100.49 kJ/mol.

Keywords: Ab initio; Car-Parrinello molecular dynamics; C −C bond; Chabazite; Constrained molecular dynamics; Coupling; Methanol; Reaction; Transition path sampling; Zeolite

1. Introduction

A major research problem in heterogeneous catalysis is to determine how solid acids such as zeolites catalyze chemical reactions. One reaction that has attracted considerable academic and industrial interest is the coupling reaction of two methanol molecules in a zeolite, to form higher chain hydrocarbons such as gasoline (MTG) or olefins (MTO) [1–22]. The MTG process was developed in the late 1970's and commercialized in 1986 by Mobil [23,24] as a response to the global energy crisis and a new interest in synfuels and other alternative gasoline sources. When the price of gasoline dropped, there was no longer a pressing need for the MTG process, however, methanol continued to be produced. Recently, interest has shifted to the MTO process, which was developed by Mobil and UOP/Norsk Hydro in 1996 [16]. Olefin and gasoline production can be coupled, since zeolites such as H-ZSM-5 and zeotypes such as SAPO-34 can oligomerize light olefins into a gasoline-like mixture of paraffins, higher olefins, aromatics, and naphthalenes.

It has been thought that the formation of the first C −C bond is the rate-limiting step of these processes, but unfortunately, the reaction or reactions comprising this process have never been isolated experimentally, nor has a mechanism been definitely agreed upon [16]. In fact, there have been over 20 proposed mechanisms for C −C bond formation. Most of these are derived from the oxonium ylide (Fig. 1(a)) or carbene (Fig. 1(b)) mechanisms, both of which involve the formation of a CH_2: moiety which can then insert itself into hydrocarbon chains. The oxonium ylide mechanism requires the prior formation dimethyl ether, forms a trimethyloxonium ion intermediate, and results in the formation of ethylene. The carbene mechanism requires the prior formation of a surface methoxy group at the zeolite acid site.

* Corresponding author.
E-mail address: trout@mit.edu (B.L. Trout).

0920-5861/$ – see front matter © 2005 Published by Elsevier B.V.
doi:10.1016/j.cattod.2005.04.005

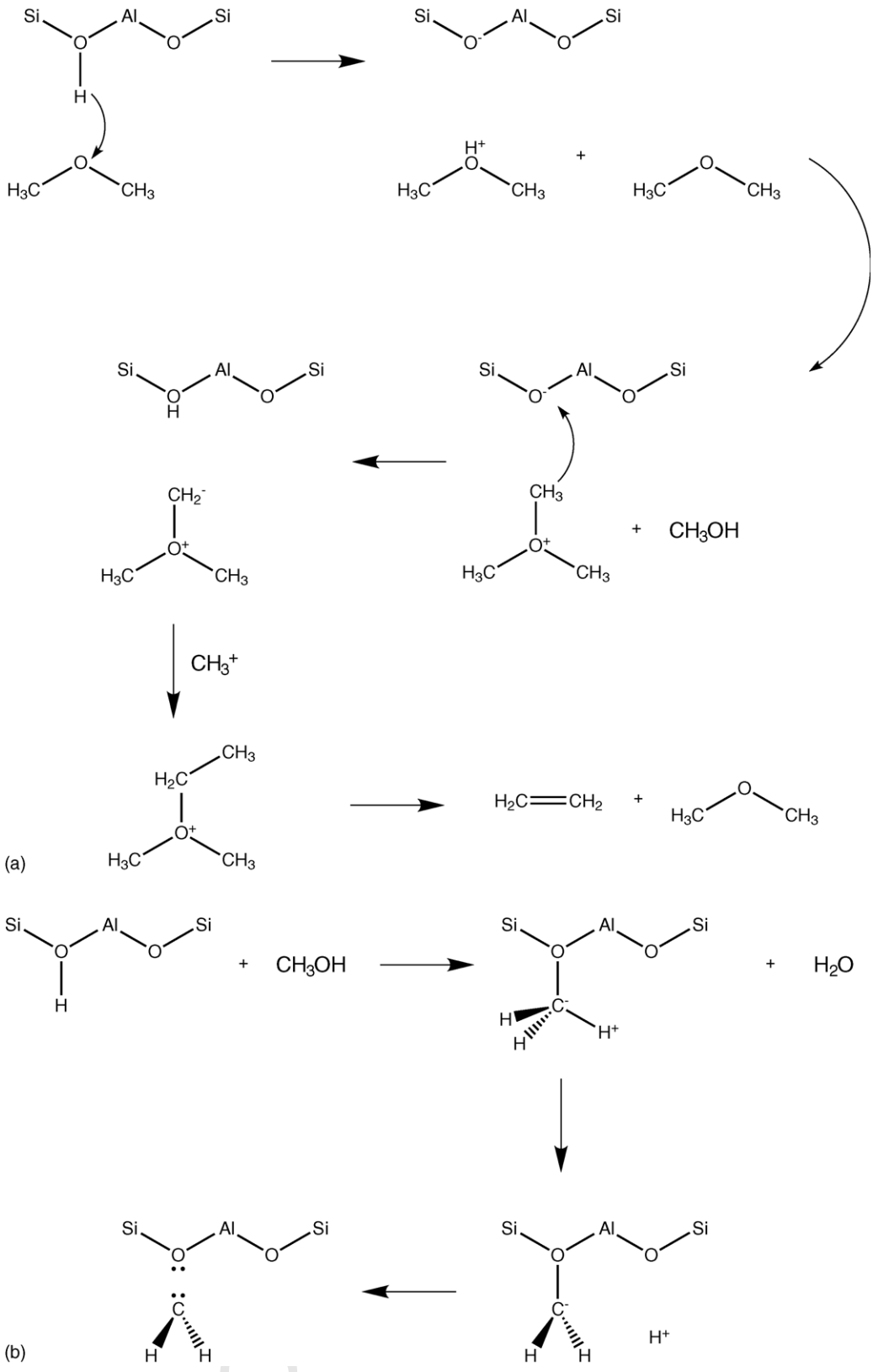

Fig. 1. Proposed mechanisms for C −C bond forming in the methanol coupling reaction, requiring the formation of (a) Oxonium ylide [57,58] and (b) carbene [23,59,60].

Recently, indirect mechanisms (Fig. 2(a)) have been proposed [22] that involve a pool of hydrocarbon species, including methylbenzenes and cyclic carbenium ions such as those in Fig. 2(b). These hydrocarbons tend to form in the pores of zeolites by the reaction of impurities in the methanol feed, and serve to stabilize the intermediates and transition states of the C −C bond forming process. In particular, the dangling methyl groups on the hydrocarbons may be the organic reaction centers, not the surface methoxy groups that have been proposed. Haw et al. [19] have recently lent support to the hydrocarbon pool mechanism by contradicting the assumption that methanol or dimethyl ether can react by themselves to form olefins in the MTO process. They fed purified methanol and dimethyl ether reagents at 375 °C over a bed of H-ZSM-5 catalyst, and found that no olefin products were formed. Only in the presence of impure methanol were ethylene and propylene formed.

To the best of our knowledge, there have been to this date only a handful of computational studies that address directly the formation of the first C −C bond [5,11,14,18]. Three of these have been performed on small cluster models using static calculations. In the first of these studies, Blaszkowski and van Santen [5] concluded that the first C −C bond is formed by the reaction of a surface methoxy group with methanol or dimethyl ether, and that pathways involving trimethyloxonium are not favorable (Fig. 3). In the second, Tajima et al. [11] proposed the ''methane–formaldehyde mechanism'' (Fig. 4), in which methanol reacts directly with a surface methoxy species to form methane and formaldehyde as stable intermediates. These then react to form ethanol, which is dehydrated to ethylene. They found that their proposed pathway is more favorable than those incorporating oxonium ylide species, carbenes, or CO. In the third, Hutchings et al. [14] proposed that the interaction of a surface methoxy species with a second methanol molecule forms a surface ethoxy species, which after β-elimination forms ethylene. In a related study, Govind et al. [18] performed static calculations on a periodic model of two methanol molecules in ferrierite, and found that a surface methoxy species reacts with methanol or dimethyl ether to form ethanol or methyl-ethyl-ether; water does not play any visible role in their mechanism (Fig. 5).

Despite the insight gained from these studies, they suffer from two major simplifications. First, the cluster calculations do not take into account the effects of the zeolite lattice, which include molecular shape selectivity, or short-range repulsions, and confinement effects, or long range attractions. Second, they do not take into account thermal effects caused by the dynamics of the motion of reactants and intermediates and entropic effects. In fact, the view of static transition-states as single saddle points can be only pictorial at best. In reality, the potential energy hypersurface would be quite rough, possessing many accessible saddle points.

In general, reaction networks for chemical processes occurring on solid surfaces are complex, involving dissociative adsorption, surface reactions, and desorption, in addition to gas phase reactions. It is also difficult to study the mechanisms of these reaction networks by isolating elementary steps, since most experimental methods determine composite properties that consist of many elementary steps lumped together, such as conversion rates and product selectivities. Therefore, computational methods that could be used to isolate and quantify elementary steps would be quite useful.

In this manuscript, we present an overview of current methods for finding reaction pathways and mechanisms, including synchronous transit methods and the nudged elastic band. We have focused on transition path sampling, which allows us to compute the lowest free energy pathway without specifying a priori the reaction coordinates. We present one of the first applications of transition path sampling, coupled with Car-Parrinello molecular dynamics, to studying a reaction of great interest to both academic and industrial researchers in heterogeneous catalysis, namely the coupling reaction of two methanol molecules in chabazite. We show the mechanism for the formation ethanol and water at 400 °C, and the activation energy for the rate limiting step of the reaction.

2. Methodology

2.1. Finding reaction pathways: current methods

There are several methods available for obtaining reaction pathways. The traditional approach has been to find transition states, or local saddle points, and then follow the imaginary mode to find the reactants and products associated with the transition state. Recent approaches such as the various synchronous transit methods have made use of a two point boundary condition, where the reactants and products are fixed, and a straight line interpolation of images or replicas of the system is initially used to connect these two states. Another method called the nudged elastic band (NEB) [25] works by simultaneously optimizing the configuration of intermediate images along the reaction pathway, which are connected to each other by springs. The method converges toward the minimum energy path (MEP) by projecting out the perpendicular component of the spring force and the parallel component of the true force acting on each image. The NEB method has been used in numerous applications, including dissociative adsorption at metal surfaces [26], diffusion of water in ice [27], and protein oxidation [28].

The NEB method is particularly useful when accurate Hessians are not available or are difficult to calculate. Convergence, however, can be slow, although new methods help to speed this up [29]. Unfortunately, both reaction mode finding and NEB give information only at a temperature of 0 K, whereas it is likely that the dynamics of the atoms and molecules at finite temperatures will affect the reaction. A

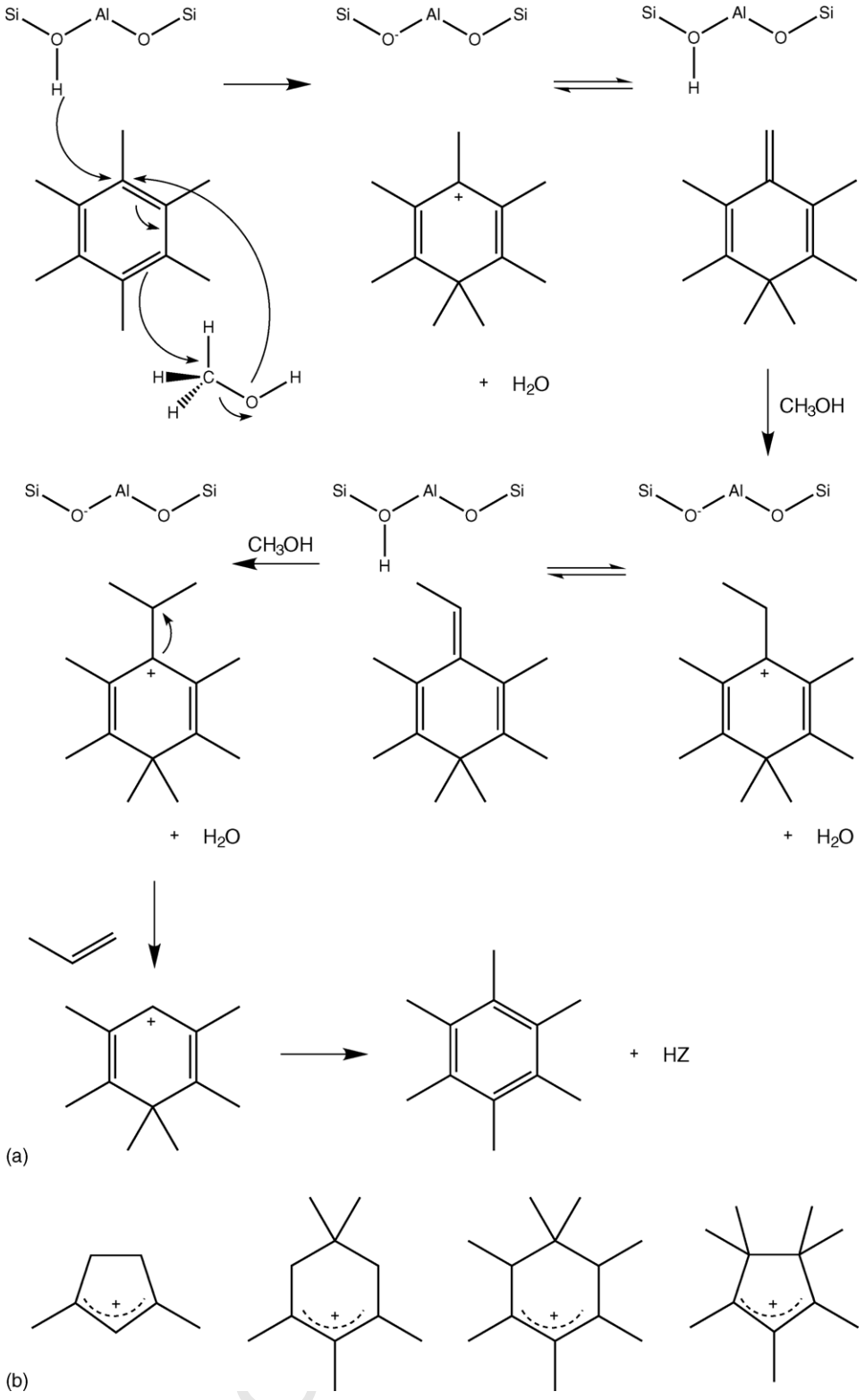

Fig. 2. (a) Proposed mechanisms for C −C bond forming in the methanol coupling reaction through an initial methylbenzene catalyst [22] and (b) possible cations in the hydrocarbon pool [61–64].

more comprehensive approach would involve sampling various dynamic pathways that are representative of the true reaction process. Transition path sampling [30–37] is such an approach.

2.2. Transition path sampling: overview

Processes in heterogeneous catalysis typically occur over timescales much larger than those directly accessible

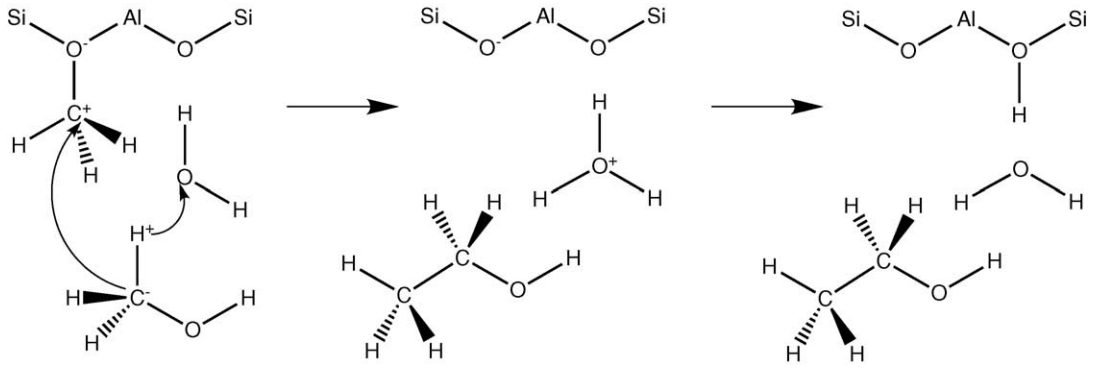

Fig. 3. C –C bond forming mechanism of Blaszkowski and van Santen [5].

via molecular simulations. While surface reactions may occur over timescales of 1 μs or larger, molecular simulation methods can probe directly timescales at only ns or even only ps, if quantum mechanical approaches are employed. This wide disparity in timescales poses serious computational difficulties for addressing these ''rare events''.

Fortunately, there are ways to bridge the problem of separation of timescales. Here, we focus on transition path sampling, a recently invented set of tools. At the core of transition path sampling is the ability to harvest an ensemble of rare trajectories that connect reactants and products within a pre-set time $\mathcal{T}$. These trajectories can be used to compute rate constants and corresponding free energy barriers, $\Delta G^{\ddagger}$, and transmission coefficients, κ, which are corrections to transition state theory. In addition, having an ensemble of rare trajectories also allows one to deduce a mechanism to describe a reaction, as we have done here for methanol coupling in a zeolite.

In order to compute rate constants accurately via transition path sampling, a large number of trajectories must be harvested. Typically, even the most powerful computers cannot accomplish this in a reasonable amount of time for complex systems. Thus, additional methods must be incorporated, and computing rate constants of complex systems is still a major research challenge. These additional methods include the blue moon ensemble [38] and umbrella sampling [39,40] approaches. We can, however, using relatively modest computational resources, harvest enough transition paths in order to identify reaction mechanisms, including unexpected intermediates.

2.3. Transition path sampling: methodology

Transition path sampling provides a means of sampling, via a Monte Carlo procedure, trajectories that connect reactants and products. In other words, transition path sampling is a random walk through the ensemble of all paths of time $\mathcal{T}$ that connect the two metastable free energy states A and B. All that is required to begin this random walk is an initial trajectory of time $\mathcal{T}$ that connects A and B. This initial trajectory can be very far from a representative pathway at the temperature of interest, but after an equilibration period, the bias in the algorithm drives the system to the most important regions of trajectory space. The result is an ensemble of dynamic paths, all of the same length, $\mathcal{T}$, which are representative of the true reaction process.

Methods such as synchronous transit and nudged elastic band are useful for finding minimum energy pathways on potential energy surfaces, which can serve as the initial trajectories for the transition path sampling algorithm. The main advantage of the Monte Carlo nature of the transition path sampling algorithm is the harvesting of an ensemble of

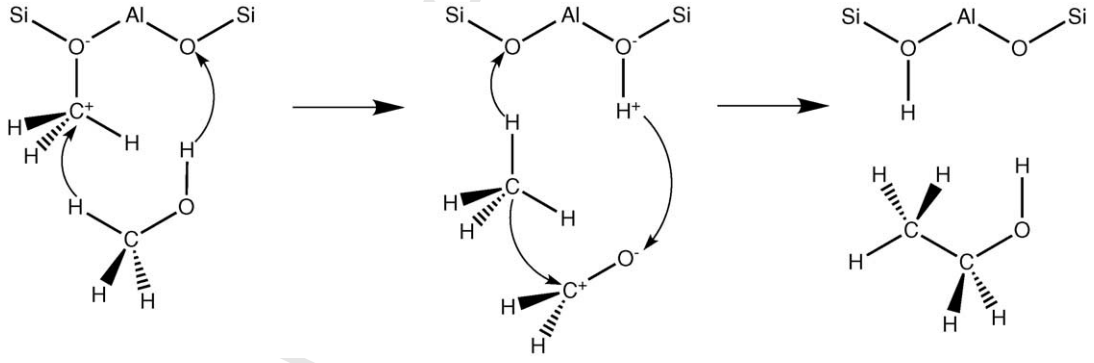

Fig. 4. C –C bond forming mechanism of Tajima et al. [11].

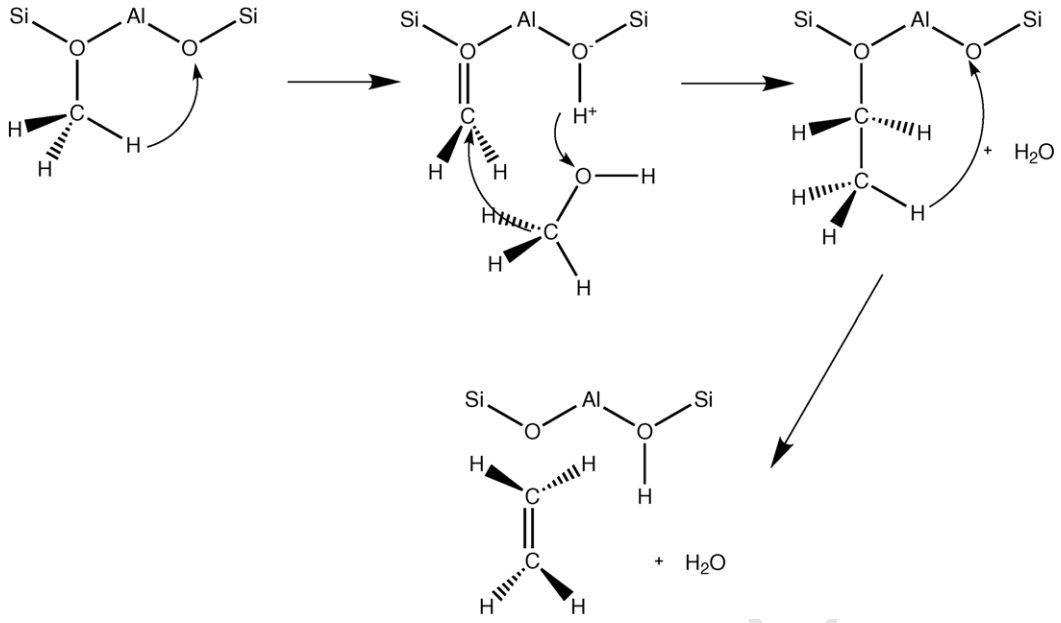

Fig. 5. C –C bond forming mechanism of Hutchings et al. [14].

pathways at the temperature of interest. There is no need to specify a priori reaction coordinates for this algorithm, so transition states and side reaction pathways that would ordinarily not be found using conventional path finding methods can be adequately sampled. Also note that there is no need for the harmonic approximation to treat degrees of freedom.

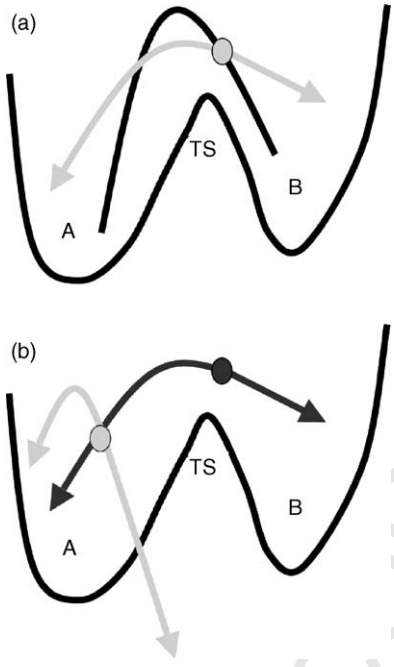

Fig. 6. Depiction of shooting algorithm for transition path sampling. (a) Initial dynamic path o (black), random time slice (gray circle) from which molecular dynamics is run forward and backward in time, and new path n (gray) connecting metastable free energy basins A and B, (b) Accepted dynamic path o (black), random time slice (gray circle), and new path n (gray), which is rejected because it does not connect A and B.

Two ways of generating new trajectories for the Monte Carlo test are shooting and shifting. In a shooting move [33], depicted in Fig. 6(a) and (b), a new transition path is created by slightly changing an existing one that connects A and B. First, a time $t$is randomly chosen on an existing path o. Second, the momentum of the system p_t^{o} is changed by a small amount δp. In practice, a random atom and random velocity component (v_x, v_y, v_z) of that atom are selected, and a new velocity component of that atom is defined such that it lies within a fixed-width Gaussian or Maxwellian distribution of the old velocity component. The velocities of all the atoms are then rescaled so that the total kinetic energy is unchanged. Then, with the new momentum of the system p_t^{n}, molecular dynamics simulations are run from t backward in time to $t = 0$ and forward in time to $t = \mathcal{T}$. The new path n is then accepted or rejected into the transition path ensemble according to a Metropolis criterion. The new trajectories conserve the total linear and angular momenta of the system, as well as maintaining detailed balance, which means that the probability of generating new momenta from the old set is the same as the reverse probability of generating the old momenta from the new set.

In the particular case where the molecular dynamics simulations are run in the microcanonical ensemble, the Metropolis acceptance probability is 100% if the new path connects A and B, as seen in Fig. 6(a), and 0% if not, as seen in Fig. 6(b). This sequence of acceptances and rejections ensures that the correct transition path ensemble is sampled. For efficient sampling, the acceptance of the new trajectories should be around 50%. This can be

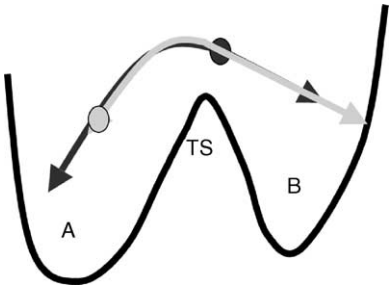

Fig. 7. Depiction of shifting move for transition path sampling. Accepted dynamic path (black), random time slice (gray circle) from which molecular dynamics is run forward in time, and new path (gray), which is the same length as the old path, and is accepted because it connects A and B.

accomplished by adjusting the magnitude of the momentum displacement δp.

The efficiency of the path sampling can also be enhanced by shifting the paths in time, as shown in Fig. 7. In a shifting move [33], a segment of length $\delta t$is deleted from either the beginning or end of an existing path o that connects A and B. A new trajectory segment of length δt is then grown from the opposite end of the path, so that the new path n is still of the same total length $\mathcal{T}$. In a forward shifting move, n is identical to o for $t = \delta t$ to $t = \mathcal{T}$, and in a backward shifting move, n is identical to o for $t = 0$ to $t = \mathcal{T} - \delta T$. Shifting only selects a slightly translated part of an existing trajectory in order to make the sampling more efficient. However, it is very useful when combined with shooting moves for facilitating convergence of path-averaged quantities. This is particularly true if the shooting algorithm is "stuck" sampling the same path over and over without generating a new accepted trajectory in the transition path ensemble.

In our system, we performed 200 iterations of the shooting and shifting algorithms, and found that this was sufficient for equilibration of the path dynamics. All shooting paths were 0.06 ps in length ($\mathcal{T}$). The simulations were run in the microcanonical ensemble, with an initial temperature of 400 °C.

2.4. Finding initial reaction paths: constrained molecular dynamics

In order to apply the transition path sampling approach, an initial dynamic path connecting A and B must be computed before the Monte Carlo algorithm can be employed. One search and optimization approach for finding initial reaction paths that we have successfully used in our group [41,42] is constrained molecular dynamics [38,43]. The advantage of this method is that only the reactants and some coordinate to drive the reaction need to be specified beforehand; the products appear over the course of the simulations, assuming that the driving coordinate was chosen appropriately. In this approach, the molecular system is taken from the reactants through the transition state to the products by applying a constraint on a putative coordinate, $q(\mathbf{r})$, that defines the progress of the reaction passing from one stable state to another; $q(\mathbf{r})$is generally chosen through chemical intuition of the relevant bond-breaking and bond-forming processes in the reaction. This coordinate can be as simple as an interatomic distance, angle, asymmetric stretch, or a many-body coordinate. At each $\xi_1 = q(\mathbf{r}_1), \xi_2 = q(\mathbf{r}_2), \ldots$, a molecular dynamics simulation is run in order to obtain an ensemble of configurations in time. In practice, for solid systems in heterogeneous catalysis, the system is initially equilibrated for about 0.5 ps before applying a Nosé-Hoover chain thermostat [44,45] on the nuclear degrees of freedom, and running a 1 ps simulation at a constant temperature. One picosecond of averaging has been found to be enough to calculate properties such as the force on the constraint with only small statistical uncertainties [42]. Even if $q(\mathbf{r})$is not the correct reaction coordinate, typically a dynamic pathway can be found by initiating unconstrained trajectories from various points along the constrained trajectories.

2.5. Calculating energetics of molecular systems

We sought to find a mechanism for C −C bond formation from methanol reactants in the zeolite chabazite, without postulating a priori intermediates. Chabazite was chosen instead of the industrially preferred H-ZSM-5 because its trigonal unit cell ($a = b = c = 9.281$ Å, $\alpha = \beta = \gamma = 94.275°$) contains only 36 atoms [46], making it tractable for ab initio calculations. Furthermore, chabazite has been shown to be catalytically active for the coupling of methanol [1]. In all of our calculations, we used a model containing 1 Al substituent per unit cell.

We used density functional theory [47–49] for our calculations, which provides the best balance of accuracy and computational cost for computing the energetics of our large and complex molecular system. The exchange-correlation energy used is the generalized gradient approximation (GGA) of Perdew and Wang [50]. Norm-conserving Troullier-Martins pseudopotentials [51] were used to reduce the computational cost relative to all-electron calculations, while maintaining an accurate net charge density for the nuclei and core electrons. A plane-wave basis set with periodic boundary conditions was used to model chabazite as an infinite crystalline system. A plane-wave cutoff of 55 Ry was used, and we sampled only the Γ point in the Brillouin zone.

We used the Car-Parrinello Molecular Dynamics [52] code, version 3.4 [53] for all of our simulations. The Car-Parrinello formulation works by describing the nuclear motion by classical mechanics, and the electronic motion is adiabatically coupled to the nuclear motion while oscillating about the ground state at each molecular dynamics time step. The advantage of this method is that the empirical interatomic pair potentials do not need to be specified beforehand, so that chemical reactions involving bond-breaking and bond-forming, which involve electronic motion, may be modelled accurately.

3. Results and discussion

3.1. Mechanism for C −C bond formation

We previously studied the methanol coupling reaction by computing an initial reaction path using constrained molecular dynamics [42]. The optimized initial configuration is two methanol molecules chemisorbed to the chabazite acid site. The putative reaction coordinate was chosen to be the C −C distance, and was constrained at several points between 3.8 and 1.8 Å; for comparison, the C −C distance of the initial configuration is 5.14 Åand the C −C distance in ethanol is 1.6 Å. All of the simulations were run at a temperature of 400 °C.

No significant chemical events occur until the C −C distance is 2.2 Å. In this trajectory, first a proton is transferred from the zeolite acid site to one of the methanol molecules, forming a methoxonium cation, which subsequently splits into a methyl cation and water, breaking the C −O bond. Then the remaining methanol transfers one of its protons to the methyl cation, forming methane and "protonated formaldehyde" (CH_2OH^+). These three intermediates are stable for at least 2.0 ps. When the C −C distance is 1.8 Å, the water extracts a proton from methane. Then, a concerted simultaneous transfer of a proton from H_3O^+ to protonated formaldehyde occurs, just as the latter transfers a proton back to the chabazite acid site, and the final formation of an ethanol-like species. When the C −C constraint is released, the C −C bond is formed and ethanol is formed. Unfortunately, we also demonstrated that the C −C distance cannot be the correct reaction coordinate to describe the entire process from reactants through the intermediates.

In the current work, we implemented the transition path sampling algorithm with the Car-Parrinello molecular dynamics approach to obtain a mechanism for ethanol and water formation from the coupling of two methanol molecules. We found two distinct steps: the breaking of the C −O bond to form H_2O, CH_4, and CH_2OH^+, and the forming of the C −C bond to form CH_3CH_2OH.

For the C −O bond breaking step, the shooting algorithm converged towards a mechanism (Fig. 8) that was very similar to what we obtained using constrained molecular dynamics with the C −C distance fixed at 2.2 Å. First, one of the methanol molecules is chemisorbed to the zeolite acid site; chemisorption, involving proton transfer from the acidic oxygen to the base, is observed only when there is more than one methanol molecule per acid site, otherwise only physisorption is observed. Next, the C −O bond of the methoxonium cation slowly stretches until it breaks, leaving water and methyl cation. The main difference was the configuration of the intermediate step, whereby a hydride ion is transferred from the second methanol molecule's CH_3moiety to the methyl cation. Most of the trajectories have in them a nearly linear $[H_2O \cdots CH_3 \cdots H \cdots CH_2OH]^+$ structure, suggesting that there is some orbital overlap facilitating the proton transfer. The intermediates H_2O, CH_4, and CH_2OH^+ are stable for at least 2.0 ps.

For the C −C bond forming step, the shooting algorithm converged towards a mechanism (Fig. 9) that was significantly different from what we obtained using constrained molecular dynamics with the C −C distance fixed at 1.8 Å. In our new mechanism, the proton transfer from methane to water occurs concurrently with the formation of the C −C bond. After some time, H_3O^+transfers a proton back to a zeolite acid site, but different from the original one. In that way, the catalyst is unchanged at the end of the reaction.

We have also plotted the variation of two reaction coordinates as a function of timestep for the trajectories in the transition path ensemble. For the first step of the reaction, the variation in C −O distance is plotted in Fig. 10(a). From this graph, we presume that configurations with C −O < 2.5 Åbelong in A, and configurations with C −O > 2.5 Åbelong in B. For the second step in the reaction, the variation in C −C distance is plotted in Fig. 10(b). From this graph, we presume that configurations with C −C distance > 1.75 Åbelong in A, and configurations with C −C distance < 1.75 Åbelong in B.

We did not observe the high-energy formation of surface methoxy groups at the chabazite acid site in any of the trajectories obtained using transition path sampling, in contrast to what was observed by other researchers [5,11,14,18] using static calculations. Although we did observe the formation of dimethyl ether in a limited number of trajectories, we did not observe the further reaction of the ether to form a C −C bond and thus higher chain hydrocarbons.

3.2. Activation energies for each step of the reaction

The activation energy $E_a(t)$ for a reaction is given by [54]:

$$E_a(t) = \frac{\langle \dot{h}_B(x_t)\mathcal{H}(x_0)\rangle^*_{AB}}{\langle \dot{h}_B(x_t)\rangle^*_{AB}} - \langle \mathcal{H}\rangle_A \quad (1)$$

where x_t is a point in phase space, including positions and momentum components, at time t and x_0 is the initial condition. $h_A(x_t)$ and $h_B(x_t)$ are step functions that equal 1 if x_t belongs to the metastable free energy states A and B, respectively, and 0 otherwise. The Hamiltonian $\mathcal{H}$ is the total energy of the system. The first term on the right hand side of Eq. (1) is averaged over the ensemble of paths starting in A and visiting B before time $\mathcal{T}$. The time derivatives of $\langle h_B(x_t)\mathcal{H}(x_0)\rangle^*_{AB}$ and $\langle h_B(x_t)\rangle^*_{AB}$ can be obtained by calculating the slope of a simple linear fit over the timesteps where the function has not plateaued. We note that the first term in the expression for E_a is therefore a constant over these timesteps. The average total energy of

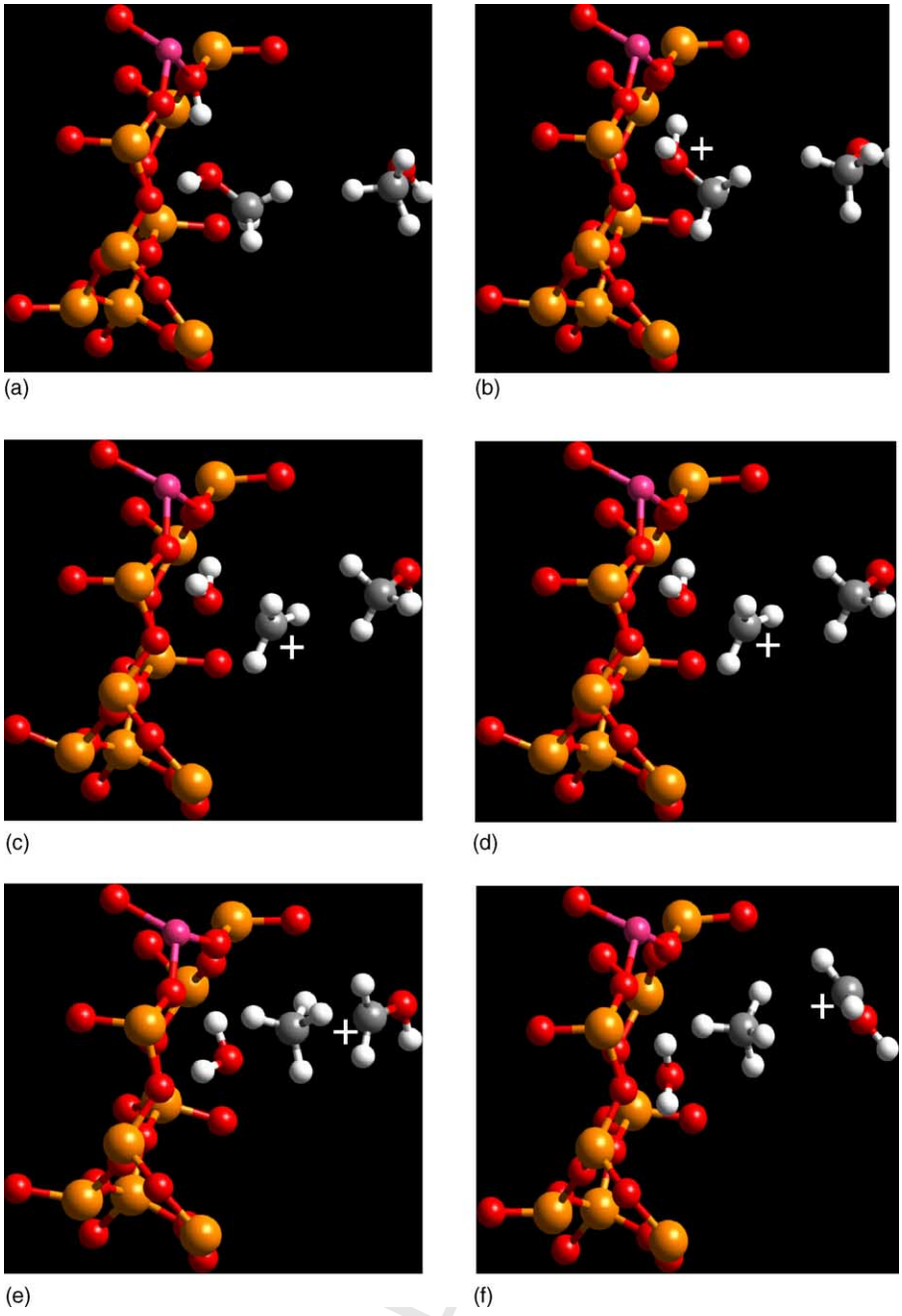

Fig. 8. Snapshots from a selected, equilibrated transition path for the first step in the methanol coupling reaction, also showing the movement of the positively charged cation. (a) Initial physisorption of methanol molecules, (b) chemisorption of methanol, with complete proton transfer from zeolite acid site to methanol, (c) breaking of C –O bond in the methoxonium cation, leaving water and methyl cation, (d) linear transition state $[H_2O \cdots CH_3 \cdots H \cdots CH_2OH]^+$ and (e) final proton transfer from methanol to methyl cation, (f) stable intermediate species H_2O, CH_4, and CH_2OH^+.

state A, $\langle \mathcal{H} \rangle_A$, is calculated from a separate molecular dynamics simulation.

The error in the calculated activation energy can be estimated from the errors in the individual terms comprising it. Since E_a can be simplified as:

$$E_a(t) = \frac{\text{term 1}}{\text{term 2}} - \text{term 3} \tag{2}$$

then:

$$\Delta(E_a) = \frac{\Delta(\text{term 1})}{\text{term 2}} - \frac{(\text{term 1}) \times [\Delta(\text{term 2})]}{(\text{term 2})^2} - \Delta(\text{term 3}) \tag{3}$$

The terms Δ(term1), Δ(term2), and Δ(term3) are found by computing the standard deviation to the linear fits.

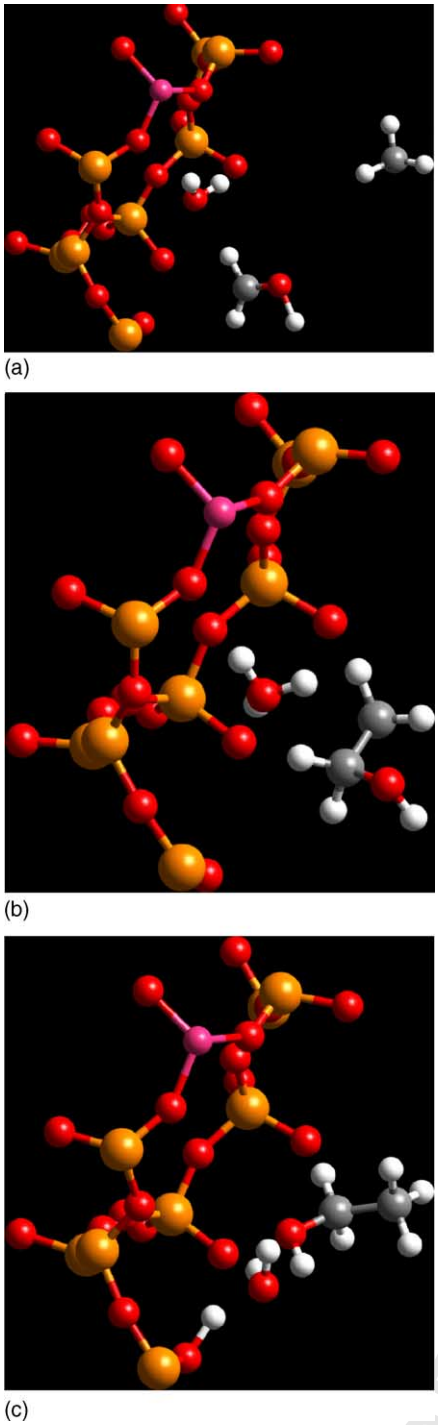

Fig. 9. Snapshots from a selected, equilibrated transition path for the second step in the methanol coupling reaction. (a) Intermediate species H_2O, CH_4, and CH_2OH^+, (b) simultaneous proton transfer from CH_4 to H_2O and formation of C −C bond, resulting in ethanol and (c) final proton transfer from H_2O back to the zeolite acid site of the adjacent unit cell, leaving the catalyst unchanged.

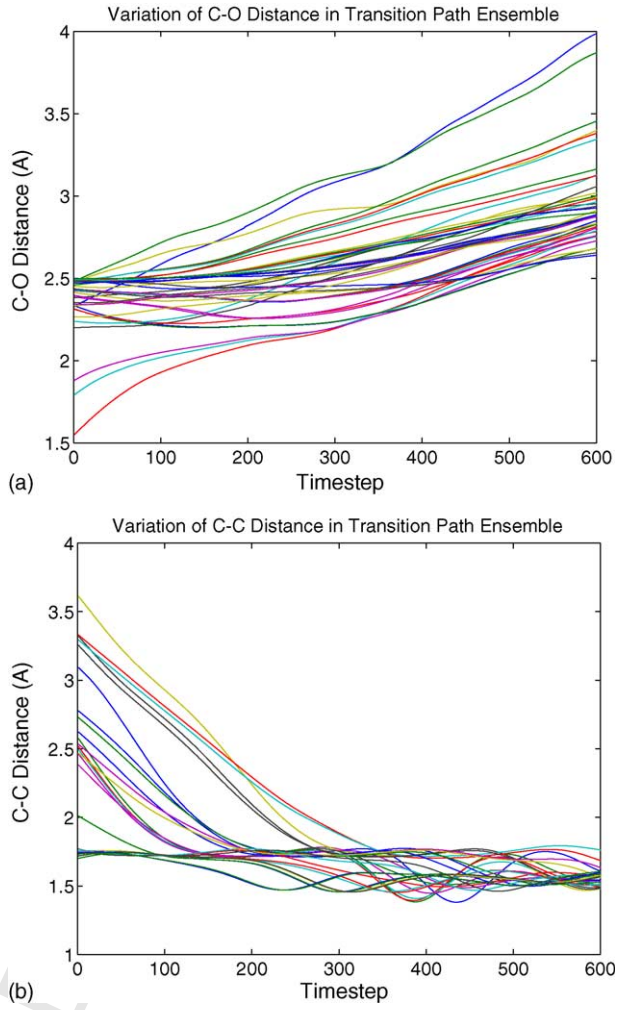

Fig. 10. Variation of (a) C −O distance and (b) C −C distance as a function of timestep for the trajectories belonging to the transition path ensemble for the two steps of the methanol coupling reaction.

For C −O bond breaking, the numerator and denominator of the first term in Eq. (1) are found by computing the slope of the graphs in Fig. 11(a) and (b), respectively. The first term comes out to be −476.96 Ha. The second term is found by averaging over the first 45 timesteps of the total energy of the system, corresponding to the initial state, as given in Fig. 12, which comes out to be −476.9725 Ha. Therefore, the overall activation energy E_a for this step is 32.78 kJ/mol, with an error of ± 18.91 kJ/mol. This error, while large, is reasonable given the small size of term 2 in the denominator of Eq. (3).

For C −C bond forming, the numerator and denominator of the first term in Eq. (1) are found by computing the slope of the graphs in Fig. 13(a) and (b), respectively. The first term comes out to be −476.9271 Ha. The second term is found by averaging over the last 200 timesteps of the total energy of the system, corresponding to the intermediate state, as given in Fig. 14, which comes out to be −476.9654 Ha. Therefore, the overall activation energy E_a for this step is 100.49 kJ/mol, with an error of ± 52.30 kJ/mol.

For comparison, the activation energy we calculated here, 100.49 kJ/mol, is much lower than that calculated previously (223.5 kJ/mol [42]), sampled across the C −C

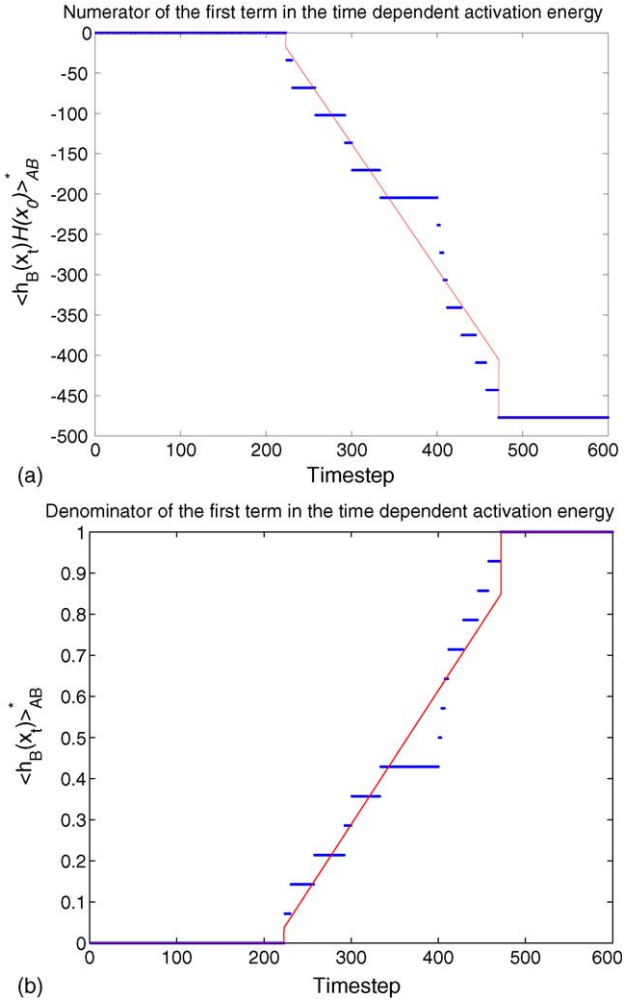

Fig. 11. Numerator and denominator of the first term in the time dependent activation energy for C −O bond breaking.

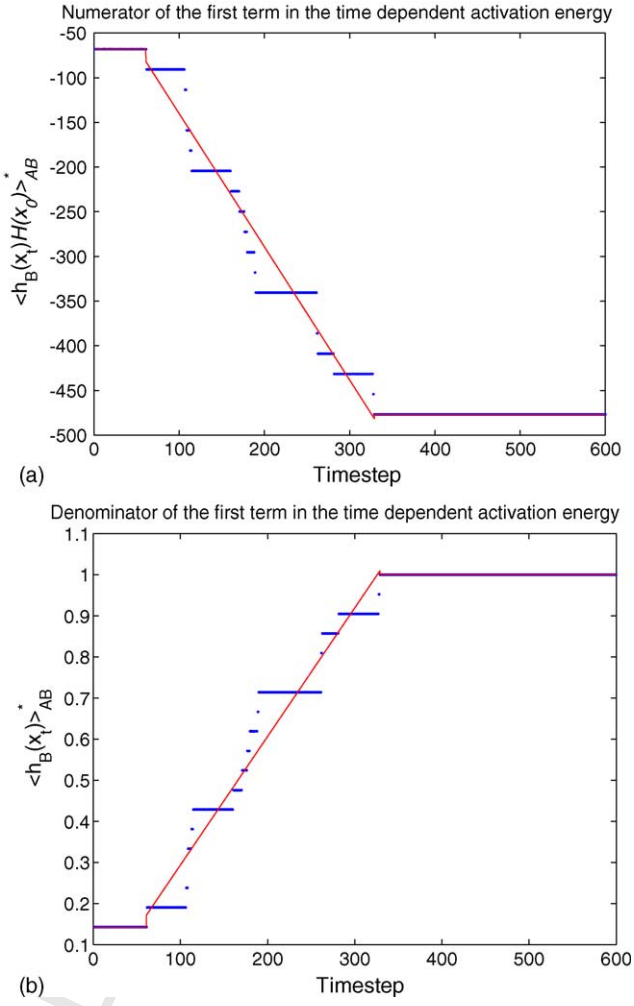

Fig. 13. Numerator and denominator of the first term in the time dependent activation energy for C −C bond forming.

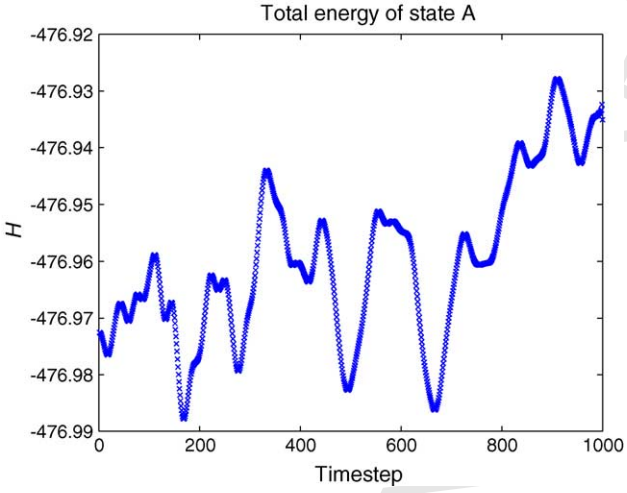

Fig. 12. Total energy of state A (two methanol reactants) for C −O bond breaking, given by averaging over the first 300 timesteps.

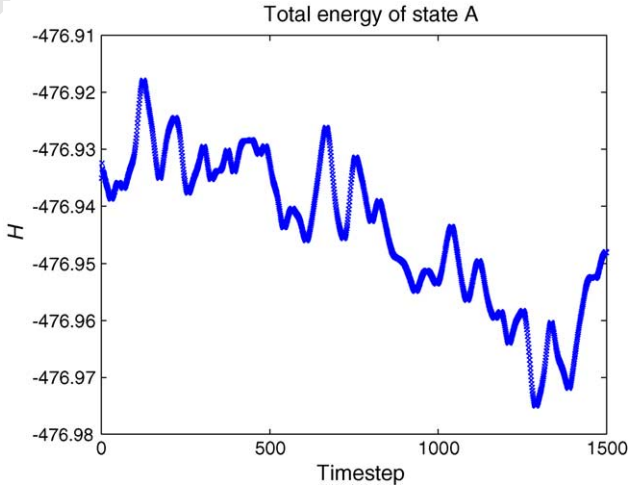

Fig. 14. Total energy of state A (H_2O, CH_4, and CH_2OH^+ intermediates) for C −C bond forming, given by averaging over the last 200 timesteps.

distance constraint using the blue moon ensemble approach [38,55]. This value, along with the corresponding internal energy $\Delta U^{TS}$of 173.8 kJ/mol, is much lower than that calculated by other researchers (183.8 kJ/mol by Tajima et al. [11] and 251.0 kJ/mol by Blaszkowski and van Santen [5]). Only limited experimental data exist for C −C bond forming reactions; 212.26 kJ/mol of thermal energy is needed for the gas phase reaction [56]:

$$[CH_3OHCH_3]^+ \rightarrow C_2H_5^+ + H_2O \quad (4)$$

4. Conclusions

We have demonstrated the application of transition path sampling and constrained molecular dynamics methods to a problem in solid state catalysis. In particular, we found a new mechanism for the C −C bond formation in the methanol coupling reaction that does not involve the formation of dimethyl ether or surface methoxy groups at the acid site. This mechanism at 400 °C proceeds through stable intermediates of water, methane, and protonated formaldehyde to form ethanol. In the first step of the reaction, the C −O bond of the chemisorbed methoxonium cation breaks, and a hydride ion is transferred from the remaining methanol molecule to the methyl cation. In the second step of the reaction, the C −C bond forms directly and concurrently with a proton transfer from methane to water. This second step is rate-limiting, since it has a higher activation energy (100.49 ± 52.30 kJ/mol) than the first step (32.78 kJ/mol).

Acknowledgements

We would like to thank the National Science Foundation for a Graduate Research Fellowship and Grant (CTS-9984301) for financial support, and the National Center for Supercomputing Applications for computing time.

References

[1] L.-T. Yuen, S.I. Zones, T.V. Harris, E.J. Gallegos, A. Auroux, Micropor. Mater. 2 (1994) 105.
[2] P.A. Barrett, R.H. Jones, J.M. Thomas, G. Sankar, I.J. Shannon, C.R.A. Catlow, J. Chem. Soc. Chem. Commun. (1996) 2001.
[3] P.E. Sinclair, C.R.A. Catlow, J. Chem. Soc., Faraday Trans. 92 (1996) 2099.
[4] S.R. Blaszkowski, R.A. van Santen, J. Am. Chem. Soc. 118 (1996) 5152.
[5] S.R. Blaszkowski, R.A. van Santen, J. Am. Chem. Soc. 119 (1997) 5020.
[6] S.R. Blaszkowski, R.A. van Santen, J. Phys. Chem. B 101 (1997) 2292.
[7] M. Bonn, R.A. van Santen, J.A. Lercher, A.W. Kleyn, H.J. Bakker, Chem. Phys. Lett. 278 (1997) 213.
[8] R. Shah, J.D. Gale, M.C. Payne, J. Phys. Chem. B 101 (1997) 4787.
[9] I. Štich, J.D. Gale, K. Terakura, M.C. Payne, Chem. Phys. Lett. 283 (1998) 402.
[10] E. Sandre, M.C. Payne, J.D. Gale, J. Chem. Soc. Chem. Commun. (1998) 2445.
[11] N. Tajima, T. Tsuneda, F. Toyama, K. Hirao, J. Am. Chem. Soc. 120 (1998) 8222.
[12] P.T. Barger, S.T. Wilson, in: M.M.J. Treacy, B.K. Marcus, M.E. Bisher, J.B. Higgins (Eds.), Proceedings of the 12th International Zeolite Conference, vol. 1, Materials Research Society, Warrendale, PA, 1999, pp. 567–574.
[13] I.M. Dahl, H. Mostad, D. Akporiaye, R. Wendelbo, Micropor. Mesopor. Mater. 29 (1999) 185.
[14] G.J. Hutchings, G.W. Watson, D.J. Willock, Micropor. Mesopor. Mater. 29 (1999) 67.
[15] G. Sastre, D.W. Lewis, in: M.M.J. Treacy, B.K. Marcus, M.E. Bisher, J.B. Higgins (Eds.), Proceedings of the 12th International Zeolite Conference, vol. 1, Materials Research Society, Warrendale, PA, 1999, pp. 341–348.
[16] M. Stöcker, Micropor. Mesopor. Mater. 29 (1999) 3.
[17] W. Song, J.F. Haw, J.B. Nicholas, C.S. Heneghan, J. Am. Chem. Soc. 122 (2000) 10726.
[18] N. Govind, J. Andzelm, K. Reindel, G. Fitzgerald, Int. J. Mol. Sci. 3 (2002) 423.
[19] W. Song, D.M. Marcus, H. Fu, J.O. Ehresmann, J.F. Haw, J. Am. Chem. Soc. 124 (2002) 3844.
[20] A. Sassi, M.A. Wildman, H.J. Ahn, P. Prasad, J.B. Nicholas, J.F. Haw, J. Phys. Chem. B 106 (2002) 2294.
[21] A. Sassi, M.A. Wildman, J.F. Haw, J. Phys. Chem. B 106 (2002) 8768.
[22] J.F. Haw, W. Song, D.M. Marcus, J.B. Nicholas, Acc. Chem. Res. 36 (2003) 317.
[23] C.D. Chang, A.J. Silvestri, J. Catal. 47 (1977) 249.
[24] C.D. Chang, J.C.W. Kuo, W.H. Lang, S.M. Jacob, J.J. Wise, A.J. Silvestri, Ind. Eng. Chem. Proc. Des. Dev. 17 (1978) 255.
[25] H. Jónsson, G. Mills, K.W. Jacobsen, B.J. Berne, G. Ciccotti, D.F. Coker, Classical and Quantum Dynamics in Condensed Phase Simulations, World Scientific, Singapore, 1998, pp. 385–404.
[26] G. Mills, H. Jónsson, Phys. Rev. Lett. 72 (1994) 1124.
[27] E.R. Batista, H. Jónsson, Comp. Mater. Sci. 20 (2001) 325.
[28] J.W. Chu, B.R. Brooks, B.L. Trout, J. Am. Chem. Soc., submitted for publication.
[29] J.-W. Chu, B.R. Brooks, B.L. Trout, J. Chem. Phys. 119 (2003) 12708.
[30] D. Chandler, B.J. Berne, G. Ciccotti, D.F. Coker, Classical and Quantum Dynamics in Condensed Phase Simulations, World Scientific, Singapore, 1998, pp. 51–66.
[31] C. Dellago, P.G. Bolhuis, F.S. Csajka, D. Chandler, J. Chem. Phys. 108 (1998) 1964.
[32] C. Dellago, P.G. Bolhuis, D. Chandler, J. Chem. Phys. 108 (1998) 9236.
[33] P.G. Bolhuis, C. Dellago, D. Chandler, Faraday Discuss. 110 (1998) 421.
[34] C. Dellago, P.G. Bolhuis, D. Chandler, J. Chem. Phys. 110 (1999) 6617.
[35] P.G. Bolhuis, C. Dellago, D. Chandler, Proc. Natl. Acad. Sci. U.S.A. 97 (2000) 5877.
[36] C. Dellago, P.G. Bolhuis, P.L. Geissler, in: Advances in Chemical Physics, vol. 123, John Wiley and Sons, 2002, pp. 4–81.
[37] P.G. Bolhuis, D. Chandler, C. Dellago, P.L. Geissler, Annu. Rev. Phys. Chem. 53 (2002) 291.
[38] E.A. Carter, G. Ciccotti, J.T. Hynes, R. Kapral, Chem. Phys. Lett. 156 (1989) 472.
[39] D. Chandler, Introduction to Modern Statistical Mechanics, Oxford University Press, New York, 1987.
[40] R. Radhakrishnan, T. Schlick, J. Chem. Phys. 121 (2004) 2436.
[41] B.L. Trout, M. Parrinello, J. Phys. Chem. B 103 (1999) 7340.
[42] C. Lo, C.A. Giurumescu, R. Radhakrishnan, B.L. Trout, Mol. Phys. 102 (2004) 281.
[43] G. Ciccotti, M. Ferrario, J. Mol. Liq. 89 (2000) 1.
[44] S. Nosé, Mol. Phys. 52 (1984) 255.

[45] G.J. Martyna, M.L. Klein, M. Tuckerman, J. Chem. Phys. 97 (1992) 2635.
[46] L.J. Smith, A. Davidson, A.K. Cheetham, Catal. Lett. 49 (1997) 143.
[47] P. Hohenberg, W. Kohn, Phys. Rev. B 136 (1964) B864.
[48] W. Kohn, L.J. Sham, Phys. Rev. A 140 (1965) A1133.
[49] R.G. Parr, W. Yang, Density Functional Theory of Atoms and Molecules, Oxford University Press, New York, 1989.
[50] J.P. Perdew, P. Ziesche, H. Eschrig, Electronic Structure of Solids '91, Akademie Verlag, Berlin, 1991, pp. 11–20.
[51] N. Troullier, J.L. Martins, Phys. Rev. B 43 (1991) 1993.
[52] R. Car, M. Parrinello, Phys. Rev. Lett. 55 (1985) 2471.
[53] J. Hutter, A. Alavi, T. Deutsch, M. Bernasconi, S. Goedecker, D. Marx, M. Tuckerman, M. Parrinello, CPMD Version 3.3 (1995–1999). Max-Planck-Institut für Festkörperforschung and IBM Zurich Research Laboratory.
[54] C. Dellago, P.G. Bolhuis, Mol. Simulat., in press.
[55] M. Sprik, G. Ciccotti, J. Chem. Phys. 109 (1998) 7737.
[56] R.D. Smith, J.H. Futtrell, Chem. Phys. Lett. 41 (1976) 64.
[57] J.P. van den Berg, J.P. Wolthuizen, J.H.C. van Hooff, L.V.C. Rees, in: Proceedings of the Fifth International Conference on Zeolites, Heyden, London, 1980, p. 649.
[58] G.A. Olah, H. Doggweiler, J.D. Feldberg, S. Frohlich, M.J. Grdina, R. Karpeles, T. Keumi, S. Inaba, W.M. Ip, K. Lammertsma, G. Salem, D.C. Tabor, J. Am. Chem. Soc. 106 (1984) 2143.
[59] C.S. Lee, M.M. Wu, J. Chem. Soc. Chem. Commun. 5 (1985) 250.
[60] J.K.A. Clarke, R. Darcy, B.F. Hegarty, E. O'Donoghue, V. Amir-Ebrahimi, J.J. Rooney, J. Chem. Soc. Chem. Commun. (1986) 425.
[61] P.W. Goguen, T. Xu, D.H. Barich, T.W. Skloss, W. Song, Z. Wang, J.B. Nicholas, J.F. Haw, J. Am. Chem. Soc. 120 (1998) 2650.
[62] T. Xu, D.H. Barich, P.W. Goguen, W. Song, Z. Wang, J.B. Nicholas, J.F. Haw, J. Am. Chem. Soc. 120 (1998) 4025.
[63] W. Song, J.B. Nicholas, A. Sassi, J.F. Haw, Catal. Lett. 81 (2002) 49.
[64] W. Song, J.B. Nicholas, J.F. Haw, J. Phys. Chem. B 105 (2001) 4317.